

Figure S1. MYC induces metabolic changes. A, heatmap of the metabolites regulated by MYC in the presence or absence of AHR. B, description of the metabolites shown in (A).

Figure S2. AHR regulates metabolic pathways in the absence of MYC. A, heatmap of the metabolic changes driven by AHR in *myc*^{-/-} + MYC rat fibroblasts. B, description of the metabolites shown in (A). C, heatmap of the metabolic changes driven by AHR in *myc*^{-/-} rat fibroblasts. D, description of the metabolites shown in (C). E-I, relative mRNA expression of *L2HGDH* and *MDH2* (E), *ADHEF1* and *D2HGDH* (F), *HGAH* (G), *UMPS* (H), and *LDHA* (I), according to our RNA-seq. J, qPCR for rat *LDHA* upon AHR knockdown. K, rat *LDHA* promoter showing AHR and MYC binding sites. Asterisks represent p-value <0.05.

Figure S3. Glycolysis in the absence of AHR. A, schematic representation of the glycolysis pathway. B, relative amounts of the glycolytic metabolites found in the LC/MS metabolomic screening in the presence or absence of MYC and AHR in rat fibroblasts normalized by the *myc*^{-/-} condition. C, relative mRNA levels of the enzymes involved in glycolysis found by RNA-seq in MYC-expressing cells 48 h after transfection with control or *AHR* siRNAs. Asterisks represent p-value <0.05. Asterisks in C-E represent p-value <0.05 in both *AHR* siRNA conditions relative to siCtrl.

Figure S4. TCA cycle and pyrimidine biosynthesis pathway in the absence of AHR. A, schematic representation of the TCA cycle pathway. B, relative amounts of the TCA cycle metabolites found in the LC/MS metabolomic screening in the presence or absence of MYC and AHR in rat fibroblasts normalized to the *myc*^{-/-} condition. C, relative mRNA levels of the enzymes involved in TCA cycle found by RNA-seq in MYC-expressing cells 48 h after transfection with control or *AHR* siRNAs. D, relative amounts of the pyrimidine metabolites found in the LC/MS metabolomic screening in the presence or absence of MYC and AHR in rat fibroblasts normalized to the *myc*^{-/-} condition. E, relative mRNA levels of the enzymes involved in pyrimidine biosynthesis found by RNA-seq in MYC-expressing cells 48 h after transfection with control

or *AHR* siRNAs. Asterisks represent p-value <0.05. Asterisks in C and E represent p-value <0.05 in both *AHR* siRNA conditions relative to siCtrl.

Figure S5. AHR is necessary for viability of GBM cells. A-B, mRNA levels of *ARNT*, *MYC*, and *MAX* in grade II, III or IV/GBM gliomas from patients whose tumor data are archived in the TCGA (A) and CGGA (B) databases. C, Western blot of LN229 and SF188 72 h after infection with an *AHR* shRNA lentiviral vector. *AHR* silencing induces cell cycle arrest, as indicated by increased expression of p27 and decreased expression of cyclin A1, and apoptosis, as indicated by cleaved PARP1 and cleaved caspase 3. D, relative proliferation of GBM9 72 h after transfection with control or *AHR* siRNA. Upper panel shows *AHR* silencing by Western blot. E, qPCR for *AHR*, *CAD*, *DHODH*, and *UMPS* in LN229 72 h after infection with a lentiviral vector containing an *AHR* shRNA. Asterisks represent p-value <0.05.

Figure S6. AHR, MYC and MAX bind to *LDHA*, *CAD*, *DHODH* and *UMPS* promoters. A, table displaying the coordinates in the hg19/human reference genome of the optimal IDR peaks found in the ChIP-seq experiments for *AHR* (ENCSR412ZDC) and *MYC* (ENCSR000EZD) deposited in the ENCODE database. B, representation of the signals and optimal IDR peaks of the ChIP-seq experiments for *AHR* (ENCSR412ZDC), *ARNT* (ENCSR029IBC), *MYC* (ENCSR000EZD) and *MAX* (ENCSR000EZF) deposited in the ENCODE database on the *CYP1A1* (*bona-fide* *AHR* target gene), *LDHA* (*bona-fide* *MYC* target gene), *CAD*, *DHODH* and *UMPS* genes. C, schematic representation of the human *LDHA* gene promoter regions showing the presence of XRE (*AHR* binding sites) or E-box (*MYC* binding sites).

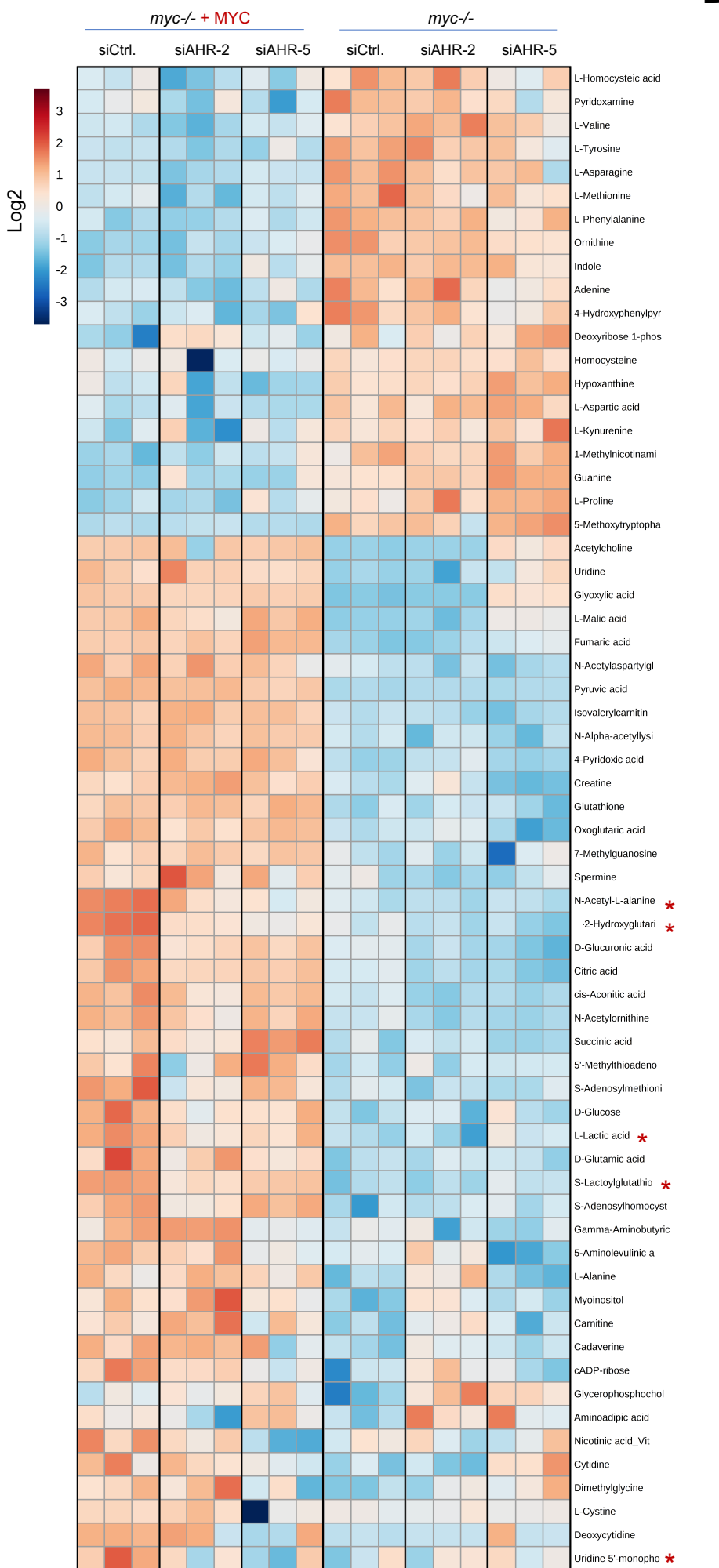
Figure S7. A, Relative amounts of the pyrimidine metabolites found in the LC/MS metabolomic screening upon *AHR* knockdown in the SF188. **B,** qPCR for *SCL28A1-3* and *SLC29A1-3* in SF188 72 h after infection with a lentiviral vector containing an *AHR* shRNA. **C-D,** Relative proliferation of SF188 (C) and *myc*^{-/-} + *MYC* (D) rat cells upon *AHR* silencing in the presence of uridine. Uridine addition did not rescue proliferation of these cells upon *AHR* knockdown.

Table S1. Antibodies, siRNA, shRNA, and primers used in this study.

Table S2. TIC values for LC/MS metabolomics in HO15.19.

Table S3. TIC values for LC/MS metabolomics in SF188.

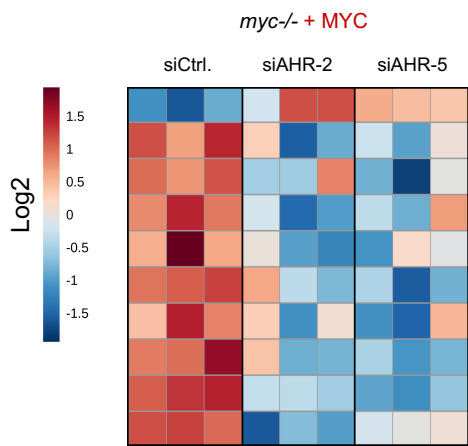
MYC-driven metabolic changes

A

B

MYC-driven metabolic changes	
Pathway	Metabolite
AA	N-Acetyl-L-alanine
	N-Alpha-acetyllysine
	L-Cystine
	L-Alanine
	L-Proline
	L-Tyrosine
	L-Valine
	L-Phenylalanine
	L-Asparagine
	L-Methionine
	L-Aspartic acid
	Alpha-aminoadipate pathway
Arginine metabolism	Creatine
Fatty acid transport	Isovalerylcarnitine
Fatty acid transport	Carnitine
Glucosaminoacids	D-Glucuronic acid
Glutaminolysis	D-Glutamic acid
Glycolysis	Pyruvic acid
	D-Glucose
	L-Lactic acid
Glyoxalase cycle	S-Lactoylglutathione
Glyoxylate cycle	Glyoxylic acid
	Acetylcholine
Methionine-Glutathione metabolism	S-Adenosylhomocysteine
	Glutathione
	5'-Methylthioadenosine
	S-Adenosylmethionine
	Dimethylglycine
	Homocysteine
Neurotransmitter	N-Acetylaspartylglutamic acid
	Gamma-Aminobutyric acid
	L-Homocysteic acid
Nicotinamide metabolism	1-Methylnicotinamide
Nucleotide synthesis	Deoxyribose 1-phosphate
Oncometabolite	2-Hydroxyglutaric acid
Phenylalanine metabolism	4-Hydroxyphenylpyruvic acid
	Myoinositol
Phospholipid	Glycerophosphocholine
Polyamine metabolism	Cadaverine
	Spermine
Porphyrins metabolism	5-Aminolevulinic acid
	7-Methylguanosine
Purines	cADP-ribose
	Adenine
	Hypoxanthine
	Guanine
	Deoxycytidine
Pyrimidines	Uridine
	Cytidine
	Uridine 5'-monophosphate
	cis-Aconitic acid
TCA cycle	L-Malic acid
	Oxoglutaric acid
	Fumaric acid
	Citric acid
	Succinic acid
Trp derivative	L-Kynurenine
	Indole
Urea cycle	5-Methoxytryptophan
	N-Acetylmornithine
Vitamin B3	Ornithine
	Nicotinic acid_Vit B3
Vitamin B6 metabolism	4-Pyridoxic acid
	Pyridoxamine

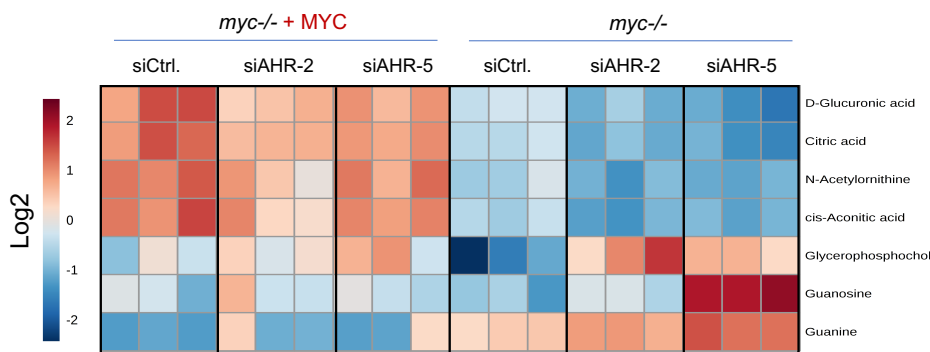
Figure S1

* AHR-driven

A**B**

AHR-driven in <i>myc</i> ^{-/-} + MYC cells	
Pathway	Metabolite
Choline metabolite	Propionylcholine
Glutathione metabolism	Pyroglutamic acid
Aminoacid	L-Histidine
Glycolysis	Lactate *
Transsulfuration pathway	L-Homoserine
Aminoacid	N-Acetyl-L-alanine *
Pyrimidines	UMP *
Vitamin B	Niacinamide
Oncometabolite	2-Hydroxyglutarate *
Glyoxalase cycle	S-Lactoylglutathione *

* Increased by MYC, downregulated by AHR

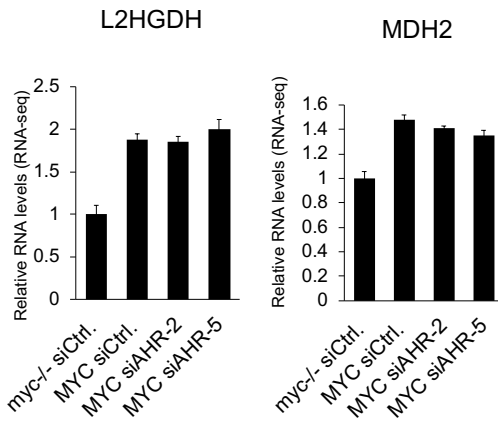
CAHR metabolic changes in *myc*^{-/-} cells**D**

AHR-driven MYC-independent metabolic changes

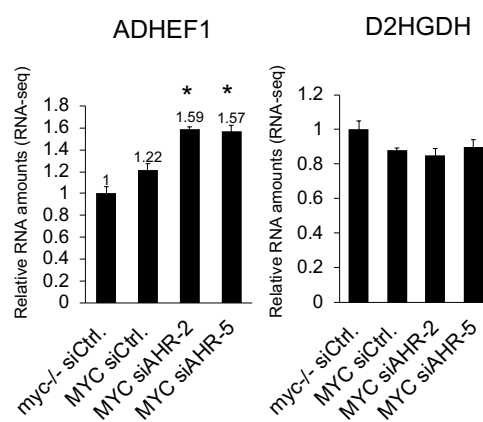
Pathway	Metabolite
Glucosaminoacids	D-Glucuronic acid
Phospholipid	Glycerophosphocholine
Purines	Guanosine
	Guanine
TCA cycle	Citric acid
	cis-Aconitic acid
Urea cycle	N-Acetylornithine

E

L-2-Hydroxyglutarate production

**F**

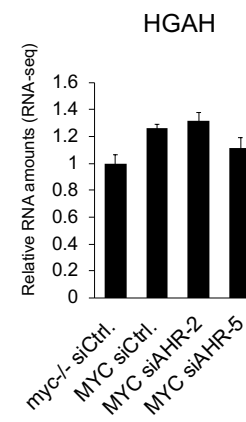
D-2-Hydroxyglutarate production



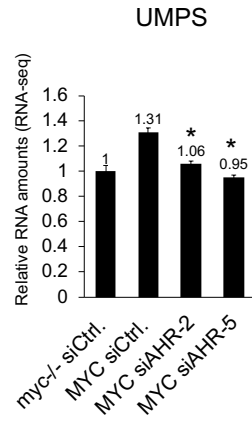
*RNA-seq showed that IDH1 and IDH2 are wild type in this rat fibroblasts

G

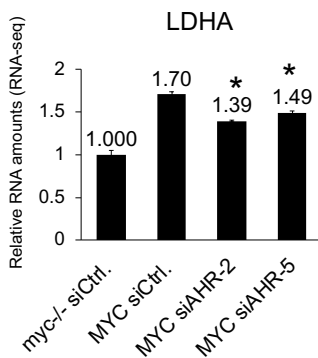
S-Lactoyl-glutathione production

**H**

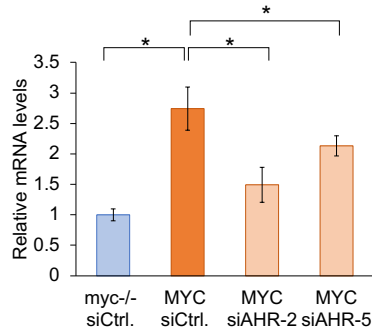
UMP production

**I**

Lactate and L-2-Hydroxyglutarate production

**J**

LDHA

**K***Rattus norvegicus*

LDHA



Figure S2

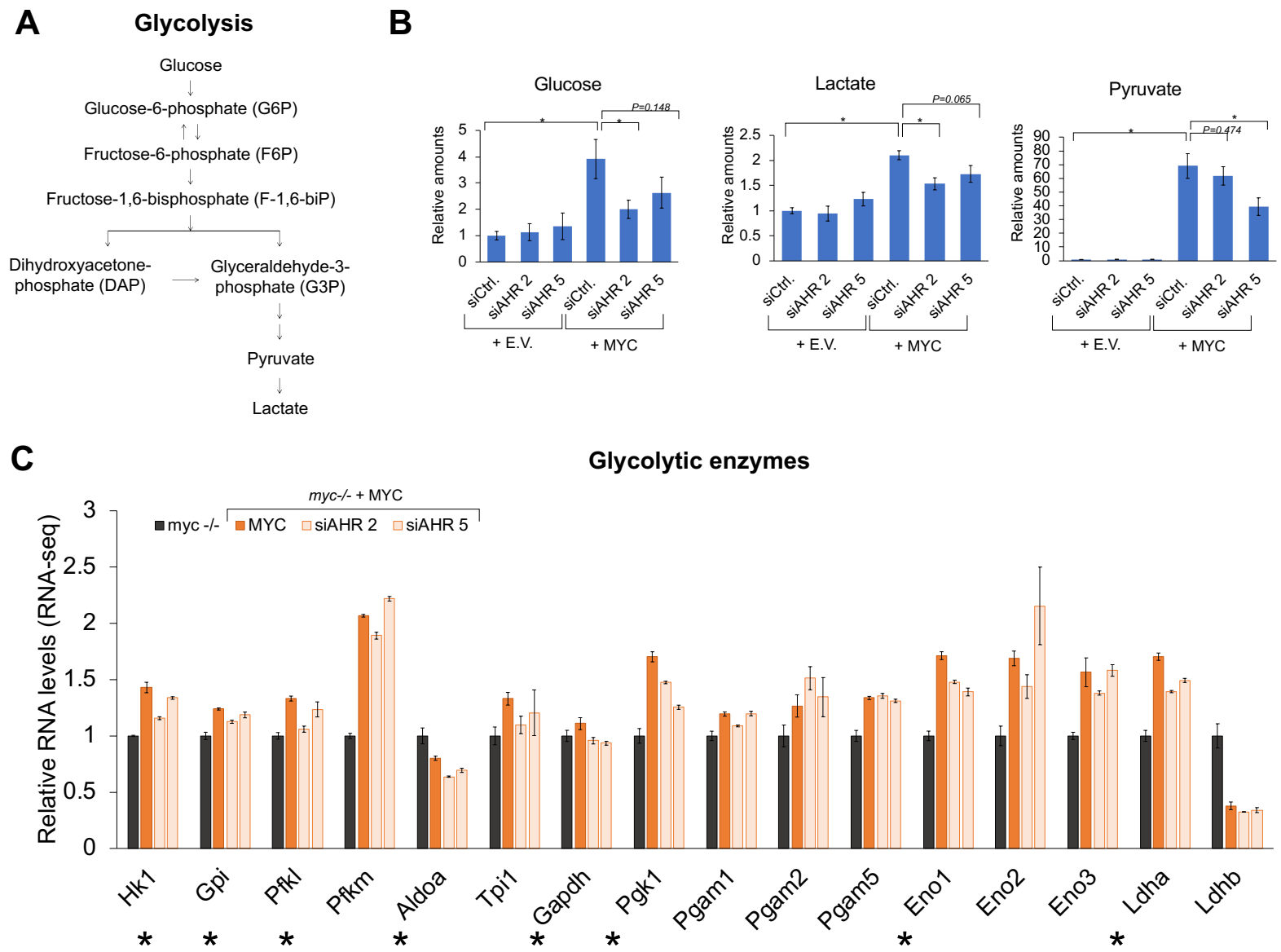


Figure S3

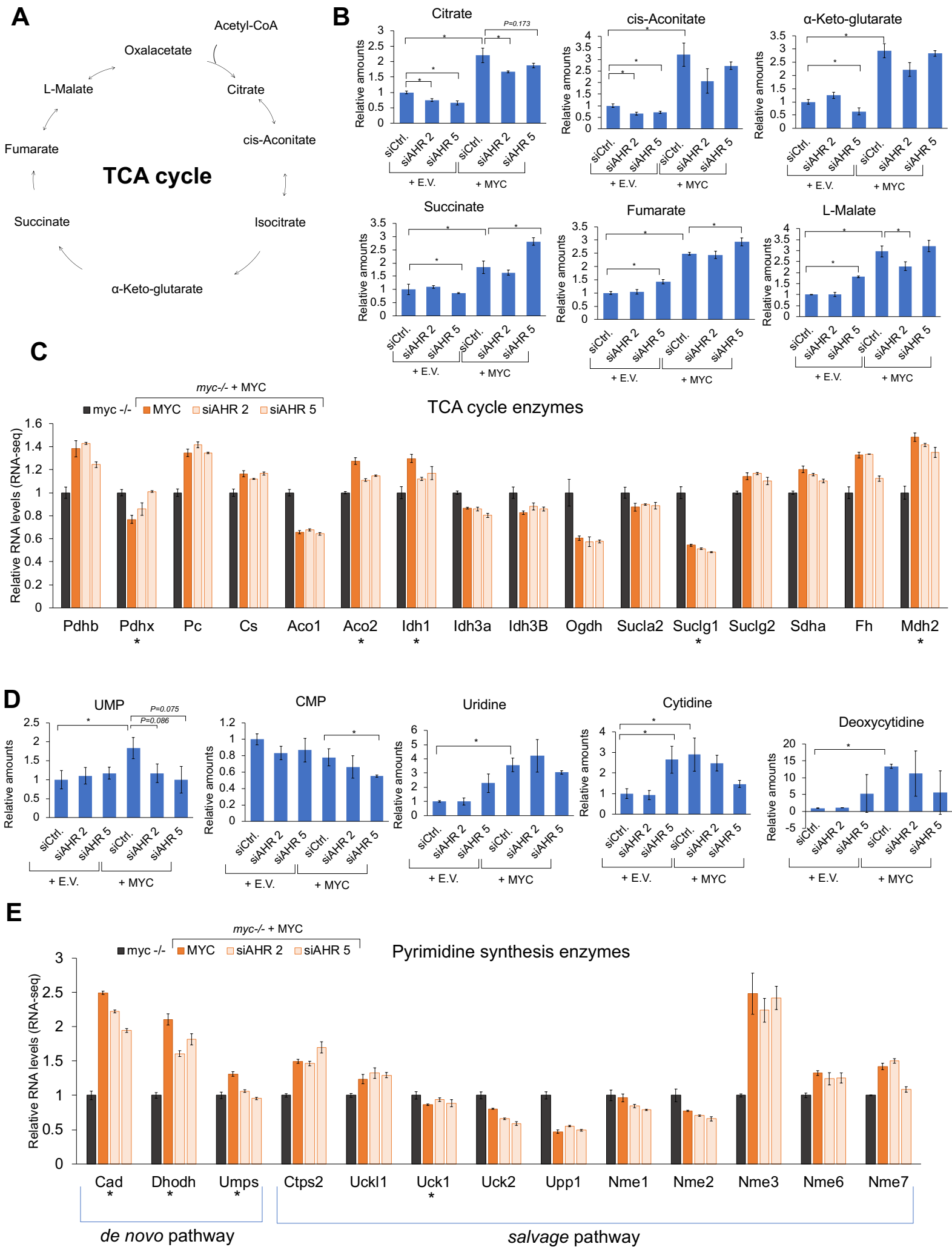
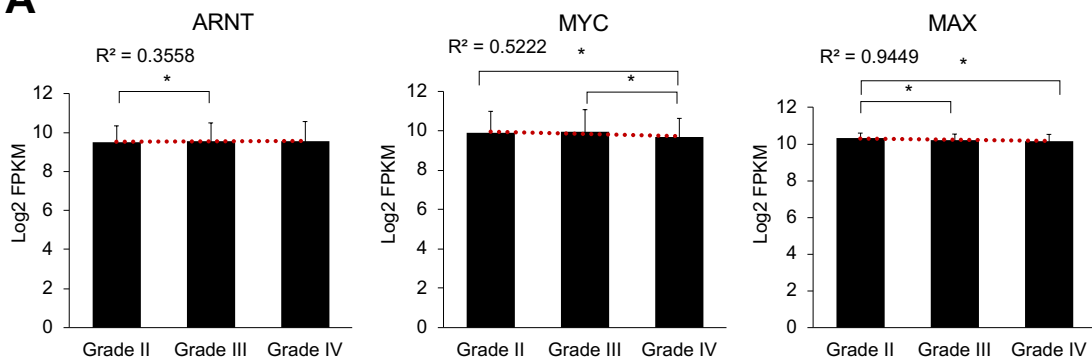
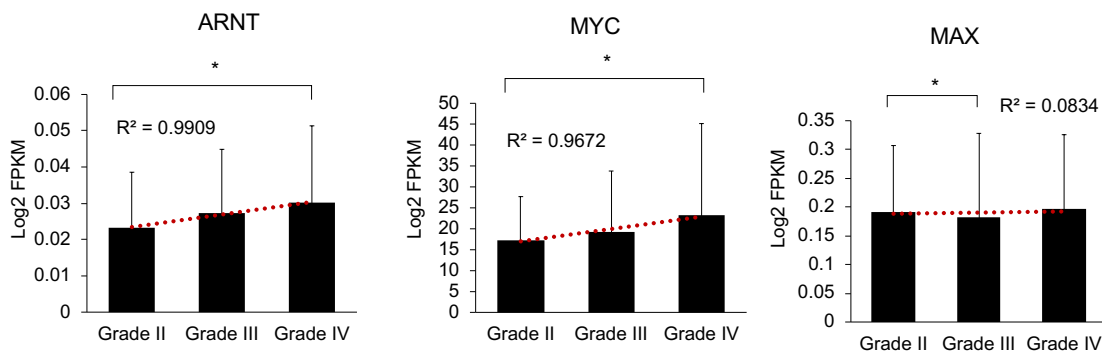


Figure S4

A**B**

Glioma patients
TCGA RNA-seq data



Glioma patients
CGGA RNA-seq data

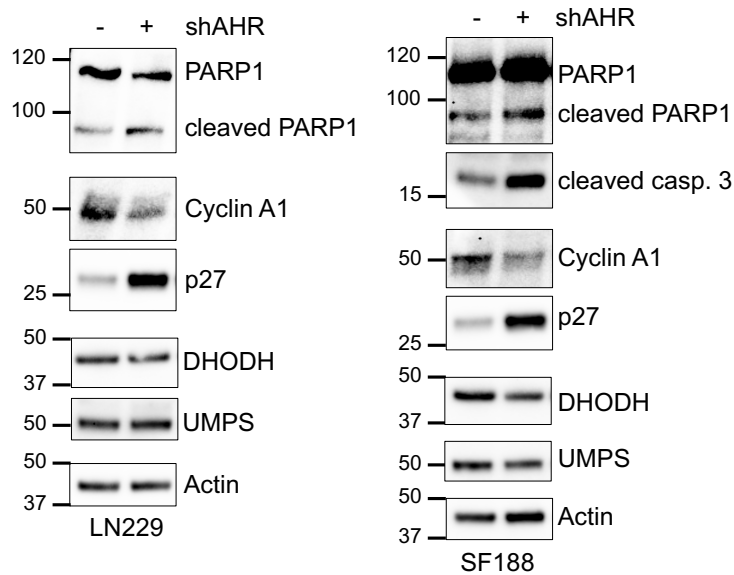
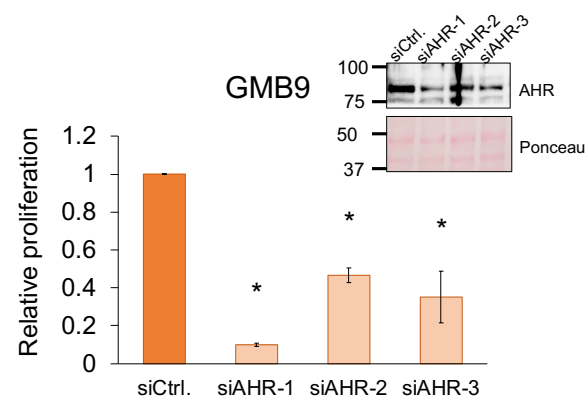
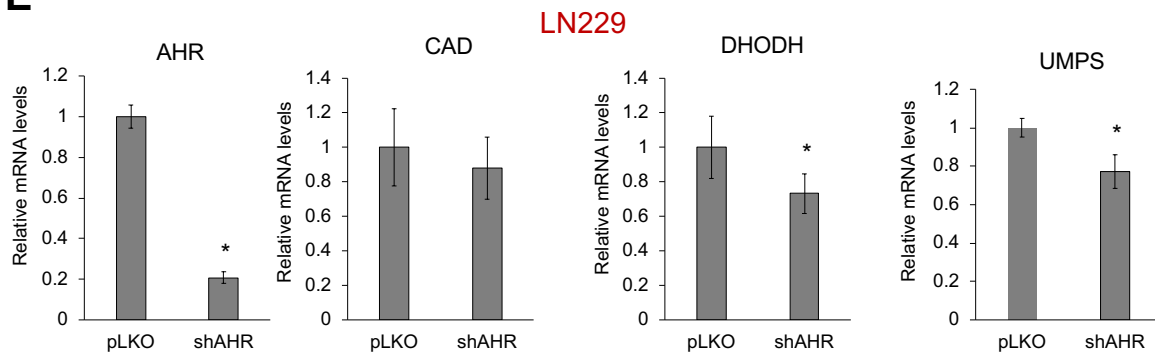
C**D****E**

Figure S5

A

hg19/Human ChIP-seq ENCODE						
Gene	AHR optimal IDR peaks (HepG2)			MYC optimal IDR peaks (HeLa-S3)		
	Coordinates	Eboxes	HRE	Coordinates	Eboxes	HRE
CAD	No peak	NA	NA	chr2:27440241-27440422	2	0
DHODH	chr16:72042582-72042997	1	4	chr16:72042486-72042829 chr16:72042686-72043029	0 1	2 3
UMPS	chr3:124449022-124449437	0	0	chr3:124449087-124449430	0	0
	chr3:124449742-124450157	0	1	chr3:124449302-124449645	0	0
	chr3:124449952-124450367	0	0			

B

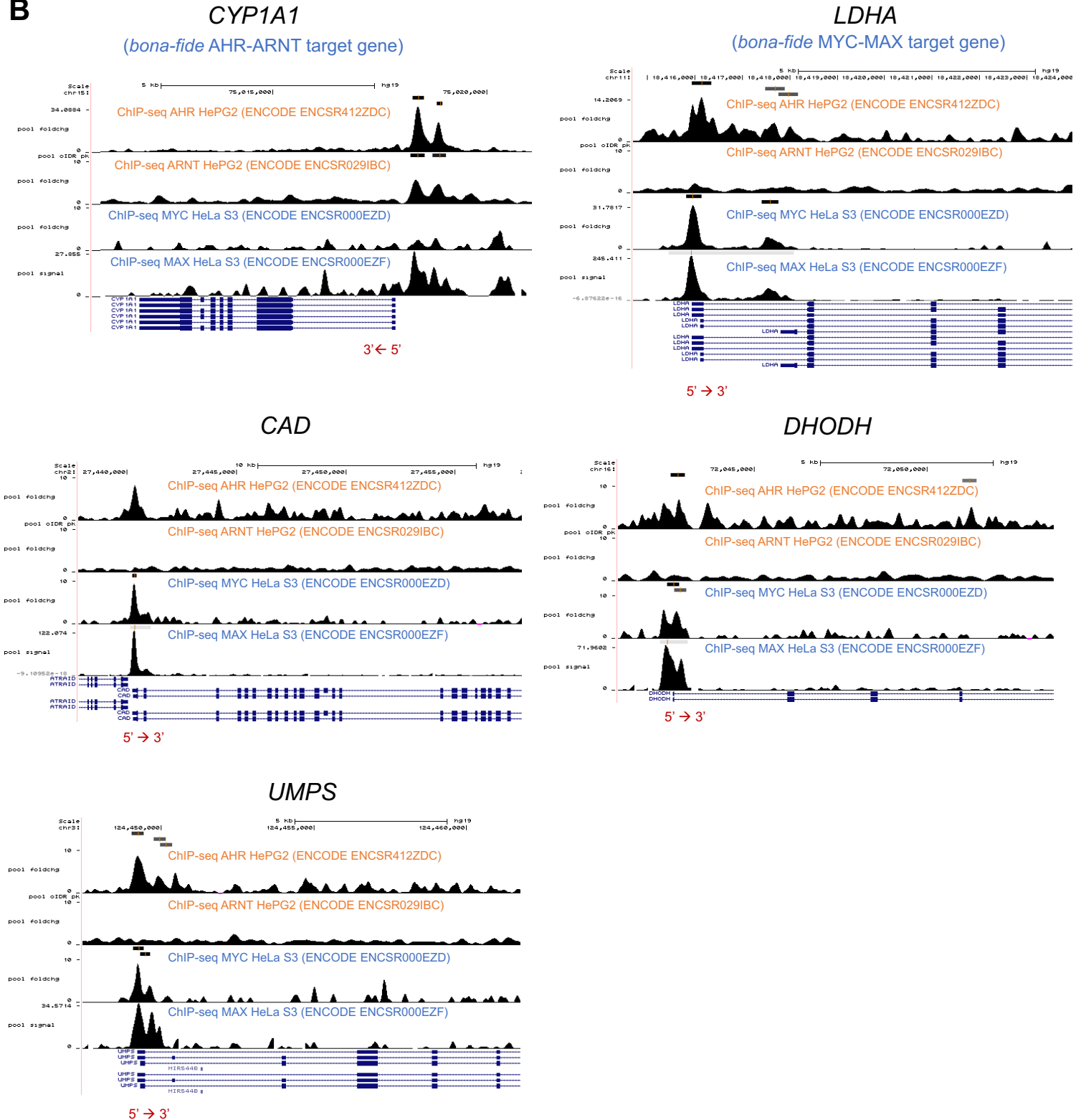


Figure S6

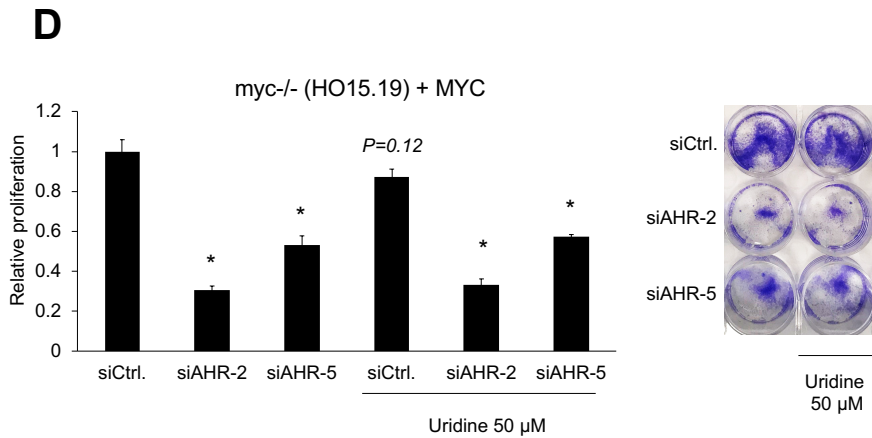
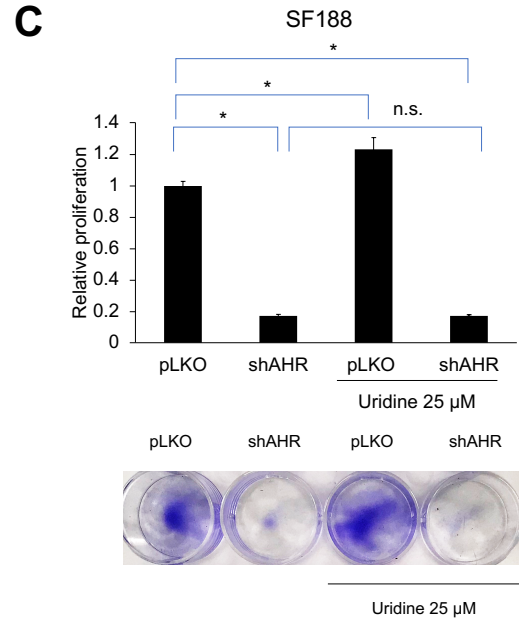
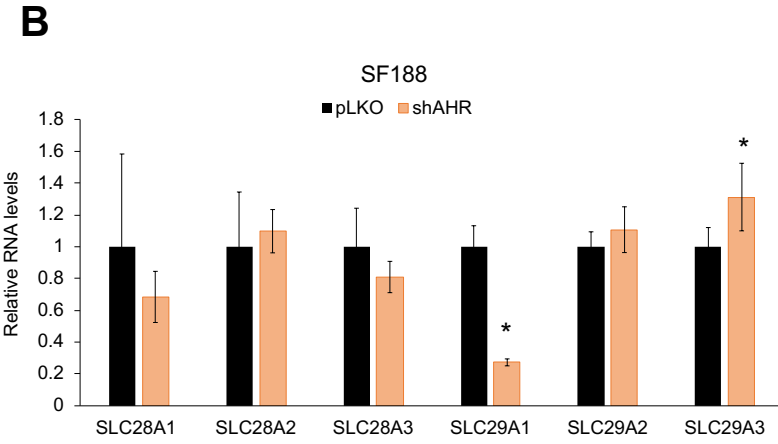
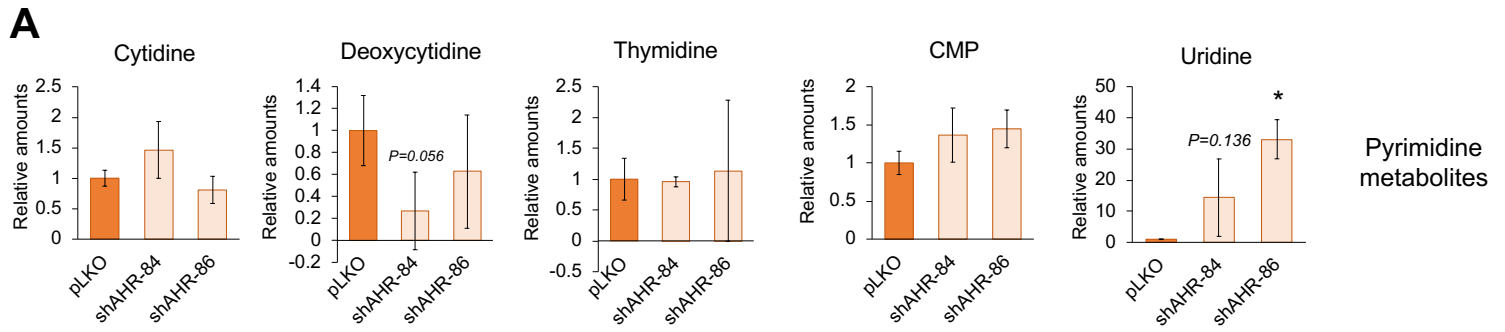


Figure S7